5-15-2007

# Utilizing Thermal Testing for Recovering

James Preciado

Thomas Werne
*Rose-Hulman Institute of Technology*

# Utilizing Thermal Testing for Recovering

**J. Preciado and T. Werne**

**Adviser: Kurt M. Bryan**

**Mathematical Sciences Technical Report Series**
**MSTR 07-03**

**May 15, 2007**

**Department of Mathematics**
**Rose-Hulman Institute of Technology**
**http://www.rose-hulman.edu/math**

**Fax (812)-877-8333** **Phone (812)-877-8193**

# Utilizing Thermal Testing for Recovering Voids in Two-Dimensional Regions

James Preciado
Thomas Werne

Rose-Hulman Mathematics REU, Summer 2006

May 15, 2007

**Abstract**

Given a two-dimensional region that contains one or more circular voids, we develop mathematical methods to locate the center and radius of the voids based on thermal boundary data. These methods can be readily applied in the field of non-destructive evaluation.

# Contents

# 1 Introduction to The Problem

The ability to ascertain the inner structure of an object without destroying the object is a useful task worth further exploration. One approach involves applying heat to the outside of the object and measuring the temperature response around the boundary. Defects or voids that may exist within the object cause variations in the boundary temperature. These differences may allow one to recover the location and size of the void(s). In this report we develop several algorithms for using the boundary temperature response induced by one or more input heat fluxes to recover the positions and areas of interior circular, perfectly insulating voids.

In our paper we build upon and use methods similar to those described in previous research. We will adapt and use the same "test function" approach for finding multiple voids as [2]; however, the method that we will describe does not need the net input flux to be zero, and only one of our methods will have the constraint of letting time be sufficiently large so that the heat in the region $\Omega$ reaches a steady state. Our research is also an extension of [4] where instead of considering cracks we examine circular, perfectly insulating voids.

## 1.1 The Forward Problem

In our problem we examine the time-dependent heat equation (1) in two spatial dimensions, where $u(x, y, t)$ is the temperature at some time $t$ for some point $(x, y) \in \Omega \subset \mathbb{R}^2$. We apply a known, controlled heat flux $g$ to the boundary $\partial\Omega$ of the region $\Omega$, modelled by equation (2) below. Inside $\Omega$ there exists a circular void $D$. For modelling purposes we assume that the boundary $\partial D$ is completely insulating (blocks all heat flow), which leads to equation (3). We also assume that the region $\Omega$ has known temperature 0 at time $t = 0$, as quantified by equation (4). The forward problem consists of using knowledge about the location and size of $D$ to solve equations (1)-(4)

and predict how the temperature will behave on the rest of $\Omega$.

$$\begin{aligned} \frac{\partial u}{\partial t} - \Delta u &= 0 \text{ in } \Omega \setminus D & (1) \\ \frac{\partial u}{\partial \vec{n}} &= g \text{ on } \partial\Omega & (2) \\ \frac{\partial u}{\partial \vec{n}} &= 0 \text{ on } \partial D & (3) \\ u(x, y, 0) &= 0 & (4) \end{aligned}$$

Of course $\Delta = \frac{\partial^2}{\partial x^2} + \frac{\partial^2}{\partial y^2}$ is the Laplacian and $\frac{\partial}{\partial \vec{n}}[f] = \nabla f \cdot \hat{n}$ on either $\partial\Omega$ or $\partial D$ is the normal derivative. We take $\hat{n}$ to point outward on $\partial\Omega$ and also outward on $\partial D$ (hence INTO $\Omega \setminus D$). Figure 1 illustrates the physical situation; the arrows indicate the applied heat flux $g$, either into or out of $\partial\Omega$.

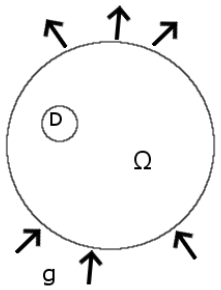


Figure 1: Single Void Problem

## 1.2 The Inverse Problem

The inverse problem is governed by the same equations (1)-(4) as the forward problem but in this case the center and the radius of $D$ are unknown. What is known, in addition to the input heat flux $g$, is the resulting induced temperature $u$ on $\partial\Omega$ over some time range $0 \leq t \leq T$.

Using techniques similar to those in [3] it can be shown that knowledge of $g$ and $u$ on any open portion of $\partial\Omega$ over any time range $t_1 < t < t_2$ uniquely determines the interior void $D$. Indeed, such measurements uniquely determine any collection of interior voids. Our task of determining $D$ from measurements of $u$ on $\partial\Omega$ is thus at least feasible.

# 2 Using Anti-symmetry to Find a Void's Center

## 2.1 The Test Function

Let $v(x, y, t)$ be a so-called "test function" that satisfies the backwards heat equation

$$\frac{\partial v}{\partial \vec{n}} + \Delta v = 0 \tag{5}$$

Let the test function also satisfy the final condition $v(x, y, T) = 0$ for some fixed time $T$. If $(p, q)$ is a point outside $\Omega$ then a particularly useful function that satisfies these conditions is

$$v(x, y, t) = \frac{1}{4\pi (T - t)} \, e^{\frac{(x-p)^2+(y-q)^2}{4(T-t)}} \tag{6}$$

## 2.2 Reciprocity Gap

We start by multiplying the heat equation by the test function $v(x, y, t)$ and then integrating with respect to time and over the region $\Omega \backslash D$. We then obtain

$$\int_{\Omega \backslash D} \int_0^T v(x, y, t) \, \frac{\partial}{\partial t} u(x, y, t) \; dt \; dA \; = \int_0^T \int_{\Omega \backslash D} v(x, y, t) \, \Delta u(x, y, t) \; dA \; dt \, . \tag{7}$$

Through integration by parts with respect to time, the left side of equation (7) becomes

$$\int_{\Omega \backslash D} v(x, y, T) \, u(x, y, T) \; dA \; - \int_{\Omega \backslash D} \int_0^T \frac{\partial}{\partial t} v(x, y, t) \, u(x, y, t) \; dt \; dA \tag{8}$$

By using the identity $v \triangle u = \nabla \cdot (v \nabla u) - \nabla u \cdot \nabla v$ the right hand side of equation (7) becomes

$$\int_0^T \int_{\Omega \backslash D} \Big( \nabla \cdot (v(x, y, t) \, \nabla u(x, y, t)) - \nabla u(x, y, t) \, \nabla v(x, y, t) \Big) \, dA \; dt \tag{9}$$

We then apply the Divergence Theorem in the plane

$$\int_S \nabla \cdot \vec{F} \, dA \; = \oint_{\partial S} \vec{F} \cdot \hat{n} \, ds$$

with $\vec{F} = v\nabla u$, where $ds$ denotes arc length, so that the expression in (9) simplifies to

$$\int_0^T \left( \oint_{\partial(\Omega \setminus D)} v\,(x,y,t)\,\nabla u\,(x,y,t) \cdot \hat{n}\, ds \; - \int_{\Omega \setminus D} \nabla u\,(x,y,t) \cdot \nabla v\,(x,y,t)\; dA \right) dt \tag{10}$$

By recombining the left and right sides of equation (7) and using the fact that $v(x,y,T) = 0$ we find

$$\int_0^T \oint_{\partial\Omega} \left( u \frac{\partial v}{\partial \vec{n}} - v \frac{\partial u}{\partial \vec{n}} \right) ds\; dt \; = \int_0^T \oint_{\partial D} u \frac{\partial v}{\partial \vec{n}}\, ds\; dt \tag{11}$$

We call this the "Reciprocity Gap" equation; it has been employed productively for the inverse problem of using impedance imaging to locate cracks, for example, in [1]. For notational convenience we define

$$\phi\,(p,q,T) \;\; := \;\; \int_0^T \oint_{\partial\Omega} \left( u \frac{\partial v}{\partial \vec{n}} - v \frac{\partial u}{\partial \vec{n}} \right) ds\; dt \tag{12}$$

so that equation (11) may be written

$$\phi(p,q,T) = \int_0^T \oint_{\partial D} u \frac{\partial v}{\partial \vec{n}}\, ds\; dt \tag{13}$$

It is extremely important to note that $\phi(p,q,T)$ can be computed from knowledge of $u$ on $\partial\Omega$, since $v$ (which we can choose) is known. By making strategic choices for $v$ we can extract information about the integral over $\partial D$ on the right in equation (13) and so glean information about $D$.

## 2.3 Observation of Anti-symmetry and Recovering the Center

Let us use polar coordinates $(r,\theta)$ based at the center of the void $D$ to expand the integral on the right in equation (13), and so obtain (using $\frac{\partial}{\vec{n}} = \frac{\partial}{\partial r}$ on

$\partial D$)

$$\begin{aligned}\phi(p,q,T) &= -\int_0^T \int_0^{2\pi} \left( u(\theta,t) \frac{(a+R\cos(\theta)-p)^2 \cos(\theta)}{8\pi (T-t)^2} \right) \\ &\quad \times \left( e^{-\frac{(a+R\cos(\theta)-p)^2+(b+R\sin(\theta)-q)^2}{4(T-t)}} \right) d\theta \; dt \\ &\quad - \int_0^T \int_0^{2\pi} \left( u(\theta,t) \frac{(b+R\sin(\theta)-q)^2 \sin(\theta)}{8\pi (T-t)^2} \right) \\ &\quad \times \left( e^{-\frac{(a+R\cos(\theta)-p)^2+(b+R\sin(\theta)-q)^2}{4T-4t}} \right) d\theta \; dt \end{aligned} \tag{14}$$

where $u(\theta,t)$ denotes $u(R,\theta,t)$ in the polar coordinate system based at the center of $D$ and $R$ is the radius of $D$.

If we assume that the radius $R$ of the void $D$ is small when compared to size of the region $\Omega$ it is reasonable to take the first term of the Taylor Series expansion of the exponential quantities in equation (14) about $R=0$, which yields

$$\begin{aligned}\phi(p,q,T) \approx &-\int_0^T \int_0^{2\pi} u(\theta,t) \frac{(a-p)\, e^{-\frac{(a-p)^2+(b-q)^2}{4(T-t)}} \cos(\theta)}{8\pi (T-t)^2} d\theta \; dt + \\ &\int_0^T \int_0^{2\pi} u(\theta,t) \frac{(b-q)\, e^{-\frac{(a-p)^2+(b-q)^2}{4(T-t)}} \sin(\theta)}{8\pi (T-t)^2} d\theta \; dt \end{aligned} \tag{15}$$

Examination of equation (15) reveals that $\phi(p,q,T)$ is approximately anti-symmetric in $(p,q)$ about $(a,b)$, that is, $\phi(a-x,b-y,T) = -\phi(a+x,b+y,T)$. Since we can compute $\phi(p,q,T)$ for all $(p,q)$ outside of $\Omega$, we should be able to use this to locate the center of anti-symmetry, that is, the center of the void $D$.

In order to recover the center of $D$ we need to identify a number of points $(p,q)$ which are anti-symmetric about $(a,b)$. This is done by performing a series of contour plots. Specifically, we find any two points $(p_1,q_1)$ and $(p_2,q_2)$ outside of $\Omega$ so that $\phi(p_1,q_1,T) = -\phi(p_2,q_2,T)$ (this isn't hard). We then construct the corresponding contours or level curves through each point and determine which two points on the two contours are farthest away from each other. This should yield points $(x_1,y_1)$ and $(x_2,y_2)$ which satisfy $\phi(x_1,y_1,T) = -\phi(x_2,y_2,T)$ and are diametrically opposite each other

through $(a, b)$. The line drawn between these points passes through the center of the void $(a, b)$. By performing this computation with several pairs $(p_1, q_1), (p_2, q_2)$ we generate lines which intersect at $(a, b)$. Moreover, inaccuracy due to experimental error in the boundary temperature measurements can be reduced by performing this process for many opposite values of $\phi$ and averaging the resulting estimates of the center $(a, b)$.

### 2.4 An Example of Anti-symmetry Method

To examine the accuracy of the center finding approach described above, we use it to find the void center of a test case where

- The domain $\Omega$ is the unit disk centered at the origin.
- The void $D$ is centered at the point $(0.6, 0.4)$ with a radius $R = 0.1$
- The heat flux applied on $\partial\Omega$ is

$$g(\theta, t) = \begin{cases} \sin(\pi t)\sin(\theta), & 0 \le t \le 1 \\ 0, & \text{else} \end{cases}$$

  for $0 \le \theta < 2\pi$, where here $\theta$ corresponds to the point $(\cos(\theta), \sin(\theta))$ on $\partial\Omega$.

- The temperature $u(x, y, t)$ was sampled at 100 uniformly spaced points on $\partial\Omega$ at 300 equally-spaced times from $t = 0$ to 3.

The forward problem is solved using FemLab. In order to compute the center we use corresponding points of anti-symmetry for 30 values of $\phi$ from $1 \times 10^{-3}$ to $2 \times 10^{-3}$ and use them to calculate estimates for the void center. We then average these estimates to arrive at an approximate void center of $(0.587, 0.425)$. Compared to the actual center at $(0.6, 0.4)$, this is an error of approximately 4%. A plot of the results can be seen in Figure 2.

## 3 Recovering the Radius via Steady State Approximation

In this section we provide an easy, fast method to find the radius of a single void $D$ in the region $\Omega$ without any knowledge of the void's location.

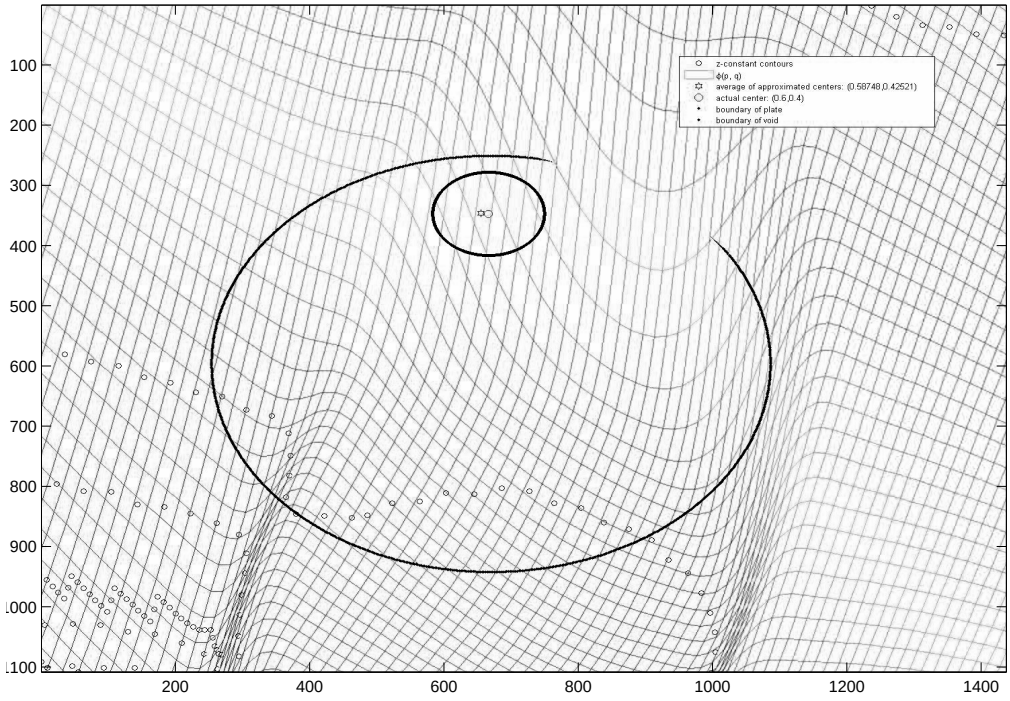


Figure 2: Locating the void center with anti-symmetry

Apply a heat flux $g$ to the $\partial\Omega$ so that a net nonzero heat energy enters the domain in a finite amount of time, that is,

$$\int_0^\infty \int_{\partial\Omega} g \, ds \, dt \neq 0.$$

As time $t \to \infty$ the temperature $u(x, y, t)$ will approach a constant steady-state temperature within $\Omega$. By using the specific heat of the material, $C_p$, the area of $D$ can be found by

$$\text{Area} = \frac{\text{net heat energy input}}{\text{measured temperature}} \, C_p = \frac{\int_0^T \oint_{\partial\Omega} g \, ds \;\, dt}{u_\infty} \, C_p$$

where $u_\infty$ denotes the (nonzero) steady-state temperature. If the region $\Omega$ is

the unit disk then

$$R = \sqrt{\frac{\pi - \text{Area}}{\pi}} \tag{16}$$

Of course this approach requires the a priori knowledge or assumption that $D$ is a disk (or other known shape).

# 4 A Second Method Using a Harmonic Test Function

In Section 2.2 we saw that if a test function $v(x, y, t)$ satisfies the backwards heat equation $\Delta v + \frac{\partial v}{\partial t} = 0$ with $v(x, y, T) = 0$ for some fixed value of $T$ then

$$\int_0^T \oint_{\partial\Omega} \left( u \frac{\partial v}{\partial \vec{n}} - v \frac{\partial u}{\partial \vec{n}} \right) ds \; dt \; = \int_0^T \oint_{\partial D} u \frac{\partial v}{\partial \vec{n}} \, ds \; dt$$

If we remove the restriction that the test function must be identically zero at a final time $T$ then the same derivation found in Section 2.2 yields the slightly modified equation

$$\begin{aligned} \int_0^T \oint_{\partial\Omega} \left( u \frac{\partial v}{\partial \vec{n}} - v \frac{\partial u}{\partial \vec{n}} \right) ds \; dt \quad &+ \quad \int_{\Omega \setminus D} u(x, y, T) \, v(x, y, T) \; dA \\ &= \quad \int_0^T \oint_{\partial D} u \frac{\partial v}{\partial \vec{n}} \, ds \; dt \end{aligned} \tag{17}$$

in which we pick up an extra term at $t = T$. Define the functional

$$\phi(v) \equiv \int_0^T \oint_{\partial\Omega} \left( u \frac{\partial v}{\partial \vec{n}} - v \frac{\partial u}{\partial \vec{n}} \right) ds \; dt \; + \int_{\Omega \setminus D} u(x, y, T) \, v(x, y, T) \; dA \tag{18}$$

so that equation (17) may be written as

$$\phi(v) \quad = \quad \int_0^T \oint_{\partial D} u \frac{\partial v}{\partial \vec{n}} \, ds \; dt \tag{19}$$

Note that unlike $\phi(p, q, T)$ from equation (12) we cannot compute $\phi(v)$ in (18) solely from knowledge of $u$ on $\partial\Omega$. However, certain approximations concerning the integral over $\Omega \setminus D$ can be made.

Without the restriction $v(x, y, T) = 0$ we have significantly more freedom in choosing a test function $v(x, y, t)$. For instance, by examining the backwards heat equation (5) it is clear that if we choose a function $v(x, y, t)$ that is time-independent then the function must be harmonic. One such class of test functions is

$$v(x, y, t) = \frac{e^{\eta(x+yi)}}{\eta} \tag{20}$$

where $\eta$ is any nonzero complex scalar. Note also that all derivatives of $v$ with respect to $\eta$ are also solutions to the backwards heat equation. These types of harmonic test functions have often been used in steady-state inverse problems.

The first integral on the right in equation (18) is calculable because we know the value of the integrand on $\partial\Omega$ for all times $t$ from 0 to $T$. We will make an approximation for the second integral. Let $u_0(x, y, t)$ denote the solution to the heat equation on $\Omega$ with input flux $g$ and no void $D$ present; note that $u_0$ is known (or can in principle be computed). We will make the approximation

$$\int_{\Omega\setminus D} u(x, y, T)\, v(x, y, T)\; dA \;\approx \int_{\Omega} u_0(x, y, T)\, v(x, y, T)\; dA\,. \tag{21}$$

We will not precisely quantify the accuracy of this approximation, but simply note that it is "intuitively" quite reasonable—if $D$ is small the $u \approx u_0$ and the integrals above ought to be close. Indeed, in the case that $v \equiv 1$ the integrals are identical. To see this note that the integral on the left in (21) when $v \equiv 1$ is

$$\begin{aligned}
\int_{\Omega\setminus D} u(x, y, T)\; dA &= \int_0^T \int_{\Omega\setminus D} u_t(x, y, T)\; dA\; dt \\
&= \int_0^T \int_{\Omega\setminus D} \triangle u(x, y, T)\; dA\; dt \\
&= \int_0^T \int_{\partial\Omega} \frac{\partial u}{\partial \vec{n}}\, ds\, dt \\
&= \int_0^T \int_{\partial\Omega} g\, ds\, dt
\end{aligned}$$

where we use $u_t = \triangle u$, the Divergence Theorem, and $\frac{\partial u}{\partial \vec{n}} \equiv 0$ on $\partial D$. Precisely the same argument (without $D$) shows that the integral on the right

in (21) has exactly the same value (essentially the total input energy from the flux) when $v \equiv 1$.

Thus given a test function $v(x, y, t)$ we now have a way to calculate an approximate numerical value for $\phi(v)$, as

$$\phi(v) \approx \int_0^T \oint_{\partial\Omega} \left( u \frac{\partial v}{\partial \vec{n}} - v \frac{\partial u}{\partial \vec{n}} \right) ds \; dt \; + \int_\Omega u_0(x, y, T)\, v(x, y, T) \; dA \quad (22)$$

Note that this approximation to $\phi(v)$ can be computed from known data.

## 4.1 Finding The Center of a Void

As shown above, we can approximately calculate a numeric value for $\phi(v)$ for any harmonic test function $v$, in particular, for $v$ as defined by (20), or for $\partial^k v / \partial \eta^k$. We would like to use this information to find the center of a void in the domain $\Omega$. In order to analyze $\phi(v)$, let's look at the right hand side of equation (19) and compute the normal derivative of the test function. For the test function $v$ we have

$$\begin{aligned} \frac{\partial v}{\partial \vec{n}} &= \nabla v \cdot \hat{n} \\ &= e^{\eta(x+yi)} \langle 1, i \rangle \cdot \left\langle \frac{x}{\sqrt{x^2+y^2}}, \frac{y}{\sqrt{x^2+y^2}} \right\rangle \end{aligned}$$

We need to compute $\frac{\partial v}{\partial \vec{n}}$ on $\partial D$, so as before we assume $D$ is a circle of radius $R$ centered at $(a, b)$, with $\partial D$ parameterized as $(x, y) = (a + R\cos\theta, b + R\sin\theta)$ for $0 \le \theta < 2\pi$. We find

$$\begin{aligned} \frac{\partial v}{\partial \vec{n}} &= e^{\eta(a+R\cos\theta+i(b+R\sin\theta))} (\cos\theta + i\sin\theta) \\ &= e^{i\theta} e^{\eta(a+bi)} e^{\eta R(\cos\theta + i\sin\theta)} \\ &= e^{i\theta} e^{\eta(a+bi)} e^{\eta R e^{i\theta}} \\ &\approx e^{i\theta} e^{\eta(a+bi)} \end{aligned} \quad (23)$$

where in the last step we assume that the radius $R$ of the void is small, so $e^{\eta R e^{i\theta}} = 1 + O(R)$.

If we change the order of integration in equation (19) and make use of (23) we obtain

$$\begin{aligned}
\phi(v) &= \int_0^T \oint_{\partial D} u \frac{\partial v}{\partial \vec{n}}\, ds\ dt \\
&\approx \int_0^T \int_0^{2\pi} u(R,\theta,t)\, e^{i\theta} e^{\eta(a+bi)} R\, d\theta\ dt \\
&\approx Re^{\eta(a+bi)} \int_0^{2\pi} \int_0^T u(R,\theta,t)\ dt\, e^{i\theta}\, d\theta
\end{aligned} \tag{24}$$

Similar analysis on $\phi\left(\frac{\partial^k v}{\partial \eta^k}\right)$ for any $k \geq 1$ yields

$$\begin{aligned}
\phi\left(\frac{\partial^k v}{\partial \eta^k}\right) &\approx R(a+bi)^k e^{\eta(a+bi)} \int_0^{2\pi} \int_0^T u(R,\theta,t)\ dt\, e^{i\theta}\, d\theta \\
&= (a+bi)^k \phi(v)
\end{aligned} \tag{25}$$

Therefore, we can approximate the center of a single void by

$$a + bi \approx \frac{\phi\left(\frac{\partial v}{\partial \eta}\right)}{\phi(v)} \tag{26}$$

## 4.2 Finding the Size of a Void

As noted in equation (24), $\phi(v)$ and $R$ are directly related. However, because we do not know the value of the temperature function $u(x,y,t)$ on $\partial D$, we cannot directly calculate $R$ from $\phi(v)$. In [2] the authors prove that in the steady-state heat conduction case one has the approximation

$$\phi(v) \approx 2e^{\eta(a+bi)} \int_0^{2\pi} \int_0^T u_0(R,\theta,t)\ dt\, e^{i\theta}\, d\theta\ + o(R^2) \tag{27}$$

where the integral itself is proportional to $R^2$. We believe that such an approximation remains valid in the time-dependent case (although we haven't fully written out the proof).

If we assume that the radius $R$ of the void is small we can use the approximation that $u_0(R,\theta,t) \approx u_0(a,b,t) + R\nabla u_0(a,b,t) \cdot \hat{n} + O(R^2)$ on $\partial D$

(easily justified with a Taylor series in the polar variable $r$) to obtain

$$\begin{aligned}
\phi(v) &\approx 2e^{\eta(a+bi)} \int_0^T u_0(a,b,t) \left( \int_0^{2\pi} e^{i\theta}\, d\theta \right) R\, dt \\
&+ 2Re^{\eta(a+bi)} \int_0^{2\pi} \left( \int_0^{2\pi} \nabla u_0\,(a,b,t) \cdot \hat{n}\; e^{i\theta}\, dt \right) R\, d\theta \\
&= 2R^2 e^{\eta(a+bi)} \int_0^{2\pi} \int_0^T \nabla u_0\,(a,b,t) \cdot \langle \cos\theta, \sin\theta \rangle\, e^{i\theta}\, dt\; d\theta \\
&= 2\pi R^2 e^{\eta(a+bi)} \int_0^T \nabla u_0\,(a,b,t) \cdot \langle 1, i \rangle\; dt \qquad (28)
\end{aligned}$$

since the integral $\int_0^{2\pi} e^{i\theta}\, d\theta$ in the first line above vanishes.

Recall that $\phi\,(v)$ is computable from the boundary data as shown in equation (18). Note also that the void center $(a,b)$ has already been determined, and so $\nabla u_0\,(a,b,t)$ is computable. We can easily find the radius $R$ of a single void $D$ from equation (28) as

$$R = \sqrt{\frac{\phi\,(v)}{2\pi e^{\eta(a+bi)} \int_0^T \nabla u_0\,(a,b,t) \cdot \langle 1, i \rangle\; dt}}. \qquad (29)$$

## 4.3 An Example

We apply the above method to an example where

- The domain $\Omega$ is the unit disk centered at the origin
- The void $D$ is centered at the point $(0.4, 0.6)$ with a radius $R = 0.1$
- The heat flux applied on $\partial\Omega$ is

$$g(\theta,t) = \begin{cases} \sin(\pi t)\sin(\theta)\,, & 0 \le \theta \le \pi/2 \;\text{ and }\; 0 \le t \le 1 \\ 0, & \text{else} \end{cases}$$

- The temperature $u\,(x,y,t)$ is sampled at 100 uniformly spaced points on $\partial\Omega$ at 100 uniformly spaced times from $t = 0$ to 1.

As in the last example the forward problem is solved using FemLab, as is the boundary value problem for $u_0$ (to compute $\nabla u_0(a,b,t)$ after the center $(a,b)$ is known). We use $\eta = 1 - 2i$ as the parameter, which yields a void center estimate of $(a,b) = (0.404, 0.592)$ and a radius estimate of $R = 0.117$. This is an error of approximately 1.2% for the center estimate and 17% for the radius estimate.

## 4.4 Dependence upon $\eta$

We find that most choices for $\eta$ yield an accurate estimate for the void center and radius. However, choosing the parameter to be close to zero frequently causes large errors in the estimate. This is likely due to the division by the parameter $\eta$ in the definition of the test function, equation (20). Closer examination shows that there are other apparent singularities in the center finding function equation (26) that we cannot explain without further analysis. Figure 3 gives an example of the dependence of these estimates on the parameter $\eta$. It is a graph of the imaginary part (or $y$ coordinate) of the estimated center from equation (26), where $\eta$ ranges over the complex domain $B = ((-5, 5) \times (-5i, 5i)) \setminus \{0\}$.

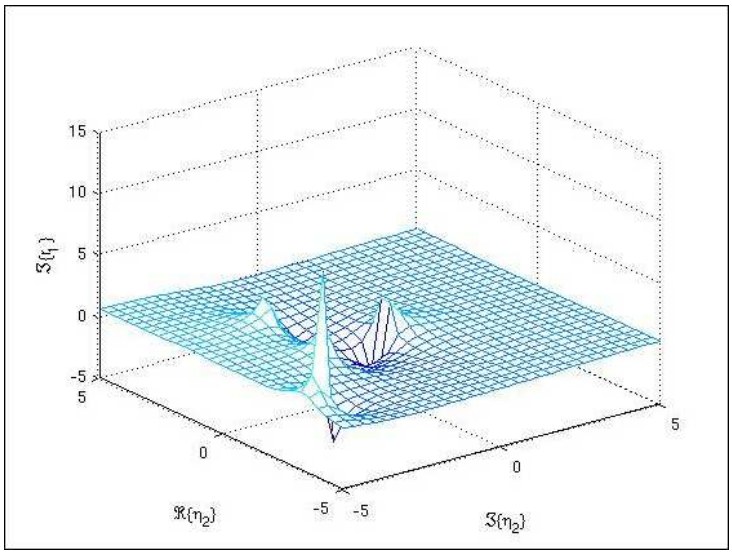


Figure 3: Imaginary Part of Center Finding Function

Of course the resulting surface should be a flat constant 0.6, but certain choices for $\eta$ yield wildly inaccurate estimates. Further analysis is necessary to better characterize this dependence.

# 5 Extension to Multiple Voids

The methods described in Section 4 can easily be generalized to a situation in which the domain $\Omega$ contains multiple voids $D_1$, $D_2$ ... $D_n$. Without loss of generality, we will proceed with the two-void derivation. The basic idea is similar to that of [4].

The forward problem is similar to the one-void case,

$$\begin{aligned} \frac{\partial u}{\partial t} - \Delta u &= 0 \text{ on } \Omega \\ \frac{\partial u}{\partial \vec{n}} &= g \text{ on } \partial\Omega \\ \frac{\partial u}{\partial \vec{n}} &= 0 \text{ on } \partial D_1 \\ \frac{\partial u}{\partial \vec{n}} &= 0 \text{ on } \partial D_2 \\ u(x, y, 0) &= 0. \end{aligned}$$

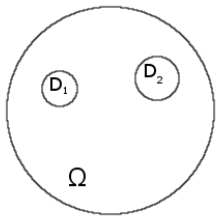


Figure 4: Two Void Problem

## 5.1 Finding the Centers of Multiple Voids

In the single-void problem we found that the functional $\phi(v)$ defined by equation (22) is approximable with the given boundary data and that

$$\phi(v) \approx \int_0^T \oint_{\partial D} u \frac{\partial v}{\partial \vec{n}} \, ds \; dt \, .$$

An analogous derivation for a two-void problem yields

$$\begin{aligned}\phi(v) &= \int_0^T \oint_{\partial D_1} u\frac{\partial v}{\partial \vec{n}}\, ds\ dt + \int_0^T \oint_{\partial D_2} u\frac{\partial v}{\partial \vec{n}}\, ds\ dt \\ &\approx J_1 e^{\eta(a_1+b_1 i)} + J_2 e^{\eta(a_2+b_2 i)}\end{aligned}$$

where

$$\begin{aligned}J_1 &= \int_0^T \oint_{\partial D_1} u(\theta,t)e^{i\theta}\, ds\ dt \\ J_2 &= \int_0^T \oint_{\partial D_2} u(\theta,t)e^{i\theta}\, ds\ dt \\ (a_1,b_1) &\text{ is the center of the void } D_1 \\ (a_2,b_2) &\text{ is the center of the void } D_2\end{aligned}$$

and as before $\theta$ denotes angular position on $\partial D$ and $\phi(v)$ is precisely as already defined by equation (22). The equations above are simply the two-void version of equation (24). We similarly find that

$$\phi(\partial^k v/\partial\eta^k) \approx J_1(a_1+b_1 i)^k e^{\eta(a_1+b_1 i)} + J_2(a_2+b_2 i)^k e^{\eta(a_2+b_2 i)}$$

analogous to equation (25).

Let $\psi(\eta)$ denote the quantity $\phi(v)$ considered as a function of the complex parameter $\eta$. We have then

$$\psi(\eta) = J_1 e^{\eta(a_1+b_1 i)} + J_2 e^{\eta(a_2+b_2 i)} \tag{30}$$

and

$$\psi^{(k)}(\eta) = J_1(a_1+b_1 i)^k e^{\eta(a_1+b_1 i)} + J_2(a_2+b_2 i)^k e^{\eta(a_2+b_2 i)}. \tag{31}$$

Note that we can compute $\psi(\eta)$ and $\psi^{(k)}(\eta)$ for any $k \geq 1$ and nonzero $\eta \in \mathbb{C}$.

Since $\psi(\eta)$ is a linear combination of two exponentials in $\eta$ it must satisfy

$$\psi''(\eta) + c_2\psi'(\eta) + c_1\psi(\eta) = 0 \tag{32}$$

for some scalars $c_1$ and $c_2$. Any such second order constant coefficient differential equation has a solution

$$\psi(\eta) = d_1 e^{r_1\eta} + d_2 e^{r_2\eta} \tag{33}$$

of the same form as equation (30). If we can determine the constants $c_1$ and $c_2$ in equation (32) we can solve the resulting ODE to obtain a solution of the form in (33). This will allow us to determine the location of the centers of the voids, since $a_k + b_k i = r_k$ (compare equations (30) and (33)). Indeed, the constants $r_1$ and $r_2$ are simply the roots $r = r_1, r = r_2$ of the characteristic equation

$$r^2 + c_1 r + c_2 = 0 \tag{34}$$

for the ODE (32).

We can determine $c_1$ and $c_2$ in equation (32) by choosing two (or more) distinct nonzero $\eta_n$ and then computing $\psi^{(k)}(\eta_n)$ for $k = 0, 1, 2$. This creates two or more linearly independent versions of equation (32) from which we can solve uniquely for the constants $c_1$ and $c_2$. We then find the roots of (34) to determine the void centers.

## 5.2 Finding the Sizes of Multiple Voids

Comparing equations (30) and (33) makes it clear that

$$\int_0^T \oint_{\partial D_k} u \, ds \; dt \; = d_k$$

By a similar derivation to that of Section 4.2, we find that

$$\int_0^T \oint_{\partial D_k} u \, ds \; dt \; = 2\pi R_k^2 \int_0^T \nabla u_0 \left(a_k, b_k, t\right) \cdot \langle 1, i \rangle \; dt \; .$$

If we determine the coefficients $d_1$ and $d_2$ in equation (33) we will obtain the radii of the two voids as

$$R_k = \sqrt{\frac{d_k}{2\pi \int_0^T \nabla u_0 \left(a_k, b_k, t\right) \cdot \langle 1, i \rangle \; dt}} \tag{35}$$

We can obtain $d_1$ and $d_2$ in a manner similar to that which yielded the values of $r_1$ and $r_2$. Specifically, we compute $\psi(\eta_1)$ and $\psi(\eta_2)$ for two distinct $\eta_k$; note that the centers $r_1 = a_1 + b_1 i$ and $r_2 = a_2 + b_2 i$ are already known. We obtain a linear system of two equation in unknowns $d_1$ and $d_2$,

$$\begin{aligned} \psi\left(\eta_1\right) &= d_1 e^{r_1 \eta_1} + d_2 e^{r_2 \eta_1} \\ \psi\left(\eta_2\right) &= d_1 e^{r_1 \eta_2} + d_2 e^{r_2 \eta_2}. \end{aligned} \tag{36}$$

We can solve this system for the variables $d_1$ and $d_2$, then substitute them into equation (35) to actually find the radii of the two voids.

It should be clear that an entirely analogous procedure can be developed for three or more voids. Moreover, one could employ the same ideas as in [4] to make an a priori estimate of the number of voids present.

## 5.3 Multiple Void Center Finding Example

We tested this algorithm with an example defined as:

- The domain $\Omega$ is the unit disk—i.e. it is a disk centered at the origin with radius $R = 1$
- The void $D_1$ is centered at the point $(0.53, 0.17)$ with radius $R = 0.18$
- The void $D_2$ is centered at the point $(0.0, -0.8)$ with radius $R = 0.07$
- The heat flux applied on $\partial\Omega$ is

$$g(\theta, t) = \begin{cases} \sin(\pi t)\sin(\theta), & 0 \leq t \leq 1 \\ 0, & \text{else} \end{cases}$$

- The temperature $u(x, y, t)$ was sampled at 100 uniformly spaced points of $\partial\Omega$ at 100 times from $t = 0$ to 1.

As in the previous example the forward problem is solved using FemLab, as is the boundary value problem for $u_0$ (to compute $\nabla u_0(a, b, t)$ after the center $(a, b)$ is known). From this data our algorithm calculated a void center estimate for $D_1$ of $(0.716, 0.390)$ and for $D_2$ of $(0.061, -0.793)$. This is an error of 51% for $D_1$ and 7.7% for $D_2$. We note that void $D_2$ is

1. smaller in radius that $D_1$
2. closer to $\partial\Omega$ than $D_2$
3. closer to the maxima of the input heat flux $g$, which occur at $\theta = \frac{\pi}{2}, -\frac{\pi}{2}$.

It may seem counterintuitive that the smaller size of $D_2$ would assist in locating the void. However, the void $D_2$'s location near the boundary of the domain *and* its proximity to the maximum heat flux make it easier to

find. And of course $D_2$ better fits the "small radius" assumption in our approximations.

We did not attempt to compute an estimate for the radii because the error inherent in the center estimates would compound itself with any error in the radius-finding algorithm.

# 6 Conclusion

We have developed several methods for characterizing voids in a bounded, two-dimensional domain $\Omega$ based upon thermal energy flow. By controlling the energy that enters the domain and measuring the temperature along the boundary we can locate the center of a single void with good accuracy by finding the center of anti-symmetry of a numerically calculable "reciprocity gap" function. Having found the center, we can then determine the size of the void $D$, at least if we allow the temperature to approach steady-state.

We also developed a second independent approach, obtained by using the reciprocity gap formula with slightly different test functions. This method yields very accurate results for a single void and has the advantage of generalizing to two or more voids. However, the second method exhibits an as yet unquantified dependence on the complex parameter $\eta$ used in the reconstruction. In certain cases, poor choice of this parameter yields extremely inaccurate (often impossible) solutions. Conversely, while the first method does not suffer from this type of problem, it requires significantly more processing time to locate the center. The second method is extremely efficient, and requires only the computation of a few boundary integrals, a couple small linear system solves, and the solution of a low-degree polynomial.

Several tasks remain. The approximations used in either method, while intuitively reasonable, are not fully justified, nor do we completely understand when they fail. A better understanding of these approximations might lead to more refined reconstruction algorithms. We would also like to implement the ideas from [4] for estimating the number of voids present, and for developing an algorithm that makes use of more than one input flux.

The last two-void example also illustrates that the input flux may significantly affect the stability with which one can locate any given void. Some analysis is in order to quantify how the input flux affects resolution. Finally, it would useful to generalize the results to non-circular voids, cracks, or even three dimensions.

# References


[1] Andrieux, S., and Ben Abda, A., *Identification de fissures planes par une donneé de bord unique; un procédé direct de localisation et d'identification*, , C.R. Acad. Sci., Paris I, 1992, **315**, pp 1323-1328.

[2] Brown, D., and Hubenthal, M., *Time dependent thermal imaging of circular inclusions*, Rose-Hulman Mathematics Technical Report 05-01, August 2005.

[3] Bryan, K., and Caudill, L., *Reconstruction of an unknown boundary portion from Cauchy data in n-dimensions*, Inverse Problems (21), 2005, pp 239-256.

[4] Bryan, K., Krieger, R., and Trainor, N., *Imaging of multiple linear cracks using impedance data*, J. of Computational and Applied Math, March 2007, Volume 200 (1), p. 388-407.